Current Biology 24, 2878–2887, December 15, 2014 ©2014 Elsevier Ltd All rights reserved http://dx.doi.org/10.1016/j.cub.2014.10.017

Article

GABAergic Modulation of Visual Gamma and Alpha Oscillations and Its Consequences for Working Memory Performance

Diego Lozano-Soldevilla,[1] Niels ter Huurne,[1,2] Roshan Cools,[1,2] and Ole Jensen[1,*]
[1]Donders Institute for Brain, Cognition and Behaviour, Radboud University Nijmegen, P.O. Box 9104, 6500 HE Nijmegen, the Netherlands
[2]Department of Psychiatry, Donders Institute for Brain, Cognition and Behaviour, Radboud University Medical Centre, P.O. Box 9101, 6500 HB Nijmegen, the Netherlands

Summary

Background: Impressive in vitro research in rodents and computational modeling has uncovered the core mechanisms responsible for generating neuronal oscillations. In particular, GABAergic interneurons play a crucial role for synchronizing neural populations. Do these mechanistic principles apply to human oscillations associated with function? To address this, we recorded ongoing brain activity using magnetoencephalography (MEG) in healthy human subjects participating in a double-blind pharmacological study receiving placebo, 0.5 mg and 1.5 mg of lorazepam (LZP; a benzodiazepine upregulating GABAergic conductance). Participants performed a demanding visuospatial working memory (WM) task.
Results: We found that occipital gamma power associated with WM recognition increased with LZP dosage. Importantly, the frequency of the gamma activity decreased with dosage, as predicted by models derived from the rat hippocampus. A regionally specific gamma increase correlated with the drug-related performance decrease. Despite the system-wide pharmacological intervention, gamma power drug modulations were specific to visual cortex: sensorimotor gamma power and frequency during button presses remained unaffected. In contrast, occipital alpha power modulations during the delay interval decreased parametrically with drug dosage, predicting performance impairment. Consistent with alpha oscillations reflecting functional inhibition, LZP affected alpha power strongly in early visual regions not required for the task demonstrating a regional specific occipital impairment.
Conclusions: GABAergic interneurons are strongly implicated in the generation of gamma and alpha oscillations in human occipital cortex where drug-induced power modulations predicted WM performance. Our findings bring us an important step closer to linking neuronal dynamics to behavior by embracing established animal models.

Introduction

The human ability to encode, maintain, and manipulate visual representations requires a strict temporal coordination of neuronal activity. Numerous investigations point to oscillatory brain activity playing an important role in cognition [1], including one of the most important cognitive operations: working memory (WM). Impressive in vitro animal models have shown that GABAergic interneurons are intimately involved in the mechanisms producing neuronal synchronization, especially the gamma band (30–100 Hz) [2, 3]. This notion is supported by exhaustive experimental work in rat hippocampus slices demonstrating that pharmacological GABAergic enhancement increases the amplitude of spontaneous gamma oscillations while decreasing the frequency [4–7]. These gamma modulations can be mechanistically explained by a prolongation of the time course of inhibitory postsynaptic currents (IPSC) caused by the GABAergic enhancement. As a consequence, the inhibitory period, which determines the gamma frequency, increases. Although these oscillatory mechanisms have been extensively investigated in animal models, such as brain-slice preparations of the rat hippocampus, the link to function is highly limited. It is not known whether the same physiological mechanisms apply to human brain oscillations and, most importantly, whether they support human WM operations.

Visuospatial WM requires the encoding and retention of neuronal representations as well as recognition. Neuronal synchronization in the gamma band has been associated with the processing of visual stimuli and attention in monkeys and humans [8]. Specifically, gamma power and coherence increase with the spatial allocation of attention ([9, 10], but see [11]) and are predictive of response times to visual stimuli [10]. On the other hand, during rest, GABAergic neurotransmission is implicated in the generation of oscillatory activity in the alpha band (8–14 Hz) in animals [12] and humans [13, 14]. Functionally, the alpha band has been linked to the allocation of computational resources by inhibiting regions not required for a given task [15, 16].

In short, recent evidence supports the notion that gamma band activity is involved in active processing, whereas alpha oscillations reflect the allocation of neuronal resources by functional inhibition. In the present study, we have used magnetoencephalography (MEG) to investigate whether the animal models for gamma and alpha oscillations generalize to humans. Here, by pharmacologically manipulating the GABAergic efficacy with lorazepam (LZP), we ask whether inhibitory interneurons are involved in producing the WM-related gamma and alpha band activity and its consequences for behavior.

Results

We performed a double-blind randomized crossover design in which healthy participants received either placebo or LZP at two different doses (0.5 mg and 1.5 mg). LZP is a common benzodiazepine that binds allosterically to $GABA_A$ receptors and enhances chloride conductance by increasing its channel-opening frequency [17]. We used MEG to measure the ongoing brain activity while subjects performed a delayed match-to-sample visuospatial WM task [18] (Figures 1A and 1B). Each trial started by presenting a centrally presented visual cue for 1.5 s. The task was to encode the sample array composed of colored squares presented in the cued hemifield while maintaining central fixation. After a 1.5 s delay interval, a probe array was presented, and participants had to indicate whether it matched the sample array or not. Prior to the MEG experiment, we had assessed the participants WM capacity.

*Correspondence: ole.jensen@donders.ru.nl

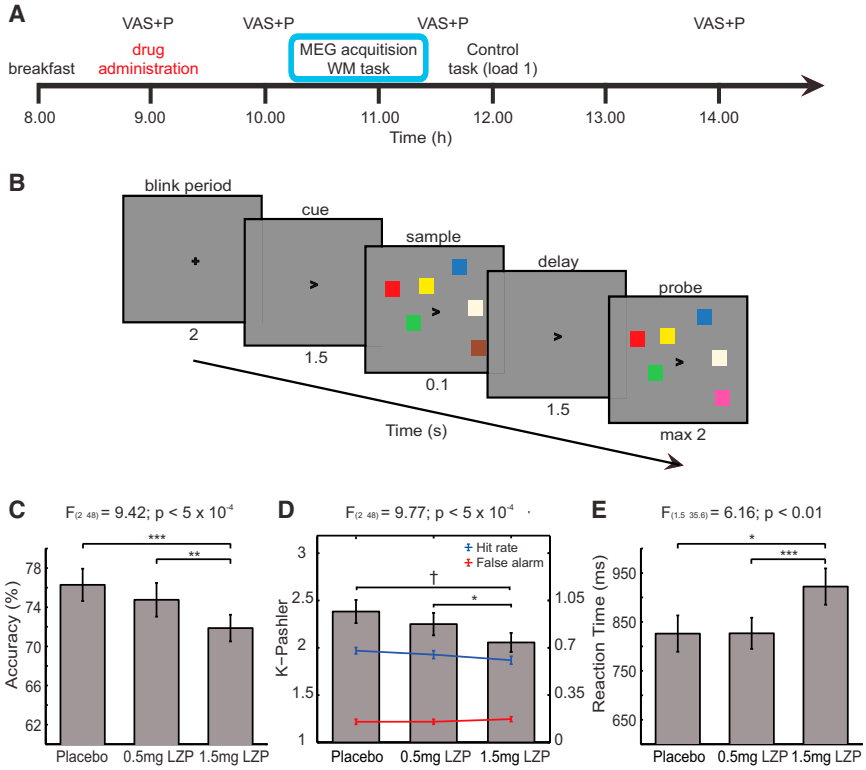

Figure 1. Experimental Design and Behavioral Results

(A) The timing of the drug administration (see Supplemental Experimental Procedures for details).

(B) The working memory (WM) task. Each trial started by presenting a cue (left or right arrow) in the center of the screen for 1.5 s. Participants had to encode a sample array of colored squares in the cued hemifield while maintaining central fixation. After a 1.5 s delay interval, a probe array was presented, and participants had to indicate whether it matched the sample array. "Match" and "nonmatch responses" were assigned using the right index and middle finger, respectively. The probe stimulus remained on the screen until the participant responded (maximum of 2 s).

(C) The accuracy (hits plus correct rejections divided by total responses) decreased as a function of drug dosage.

(D) The K_{span} (Pashler), an index that estimates the memory span when considering the errors, decreased with drug dosage. The hit and false alarm rates are also shown as blue and red lines, respectively (right y axis scale).

(E) The reaction times increased as a function of drug dosage.

LZP, lorazepam; VAS, visual analog scale; P, physiological measure (blood pressure and pulse rate).

*p < 0.05, **p < 0.01, ***p < 0.005, †$p < 5 \times 10^{-4}$. Error bars show the SEM.

This allowed us to have the participants perform with accuracy close to 75%, matching task difficulty (for details, see Supplemental Experimental Procedures available online).

Importantly, head position showed no systematic differences over the three experimental sessions ($F_{2, 48} = 0.69$, $p = 0.45$; Figure S1; see Supplemental Experimental Procedures and [19]). Although performance decreased with LZP, (see below), it did not influence performance in a control task (WM load 1, Figure S2) or drowsiness as measured by subjective questionnaire tests as a function of dosage (visual analog scales or the placebo-drug scale, Figure S3).

LZP Decreases Performance and WM Capacity

We first set out to investigate the behavioral consequences of LZP. Performance was assessed by considering K_{span} (a measure of the effective memory span when considering hits and false alarm rates) and accuracy (Figure 1C). Regarding the K_{span}, we found a strong main effect of drug ($F_{2, 48} = 9.77$, $p < 5 \times 10^{-4}$; placebo = 0.5 mg LZP: $t_{24} = 1.73$, $p = 0.09$; placebo > 1.5 mg LZP: $t_{24} = 4.39$, $p < 0.001$; 0.5 mg LZP > 1.5 mg LZP: $t_{24} = 2.7$, $p < 0.02$; Figure 1D), explained by a decrease in hit rate ($F_{2, 48} = 9.78$, $p < 5 \times 10^{-4}$) without false alarm rate change with LZP ($F_{2, 48} = 1.14$, $p = 0.33$; Figure 1D). As expected, LZP resulted in an increase in reaction times ($F_{1.5, 35.6} = 6.16$, $p < 0.01$; placebo = 0.5 mg LZP: $t_{24} = -0.02$, $p = 0.98$; placebo < 1.5 mg LZP: $t_{24} = -2.43$, $p < 0.05$; 0.5 mg LZP < 1.5 mg LZP: $t_{24} = -3.88$, $p < 0.005$; Figure 1E). Similarly, LZP decreased d prime without impact response bias (Figure S4). In conclusion, LZP produced a WM performance impairment accompanied by an increase in reaction times.

LZP Increases Stimulus-Induced Gamma Power

Here, we asked whether GABAergic neurotransmission plays a role in the generation of human gamma activity by characterizing how stimulus-induced gamma activity as measured by MEG is affected by LZP. First, we calculated the time-frequency representations (TFRs) of power in the gamma band (40–150 Hz). We observed strong stimulus-induced gamma activity over occipital sensors in response to the sample (0.1–0.35 s) and probe (1.75–2.15 s) periods in all drug conditions (Figures 2A–2C). Using a beamformer approach, we localized the sources of the gamma activity to occipital cortex with maxima in primary visual cortex.

Next, we asked whether the stimulus-induced gamma band activity was modulated by LZP by considering a set of posterior sensors (marked sensors in Figure 2 topography plots; see Supplemental Experimental Procedures for sensor selection). We constructed pairwise scatterplots comparing the different drug conditions over participants (Figure 2D). Clearly, LZP increased the stimulus-induced gamma power during the probe period in most participants, as also confirmed by a Wilcoxon signed-rank test. Also, during the sample interval, the LZP resulted in an increase in stimulus-induced gamma power ($F_{2, 48} = 3.75$, $p < 0.05$; placebo < 0.5 mg LZP: $t_{24} = -2.29$, $p < 0.05$; placebo < 1.5 mg LZP: $t_{24} = -2.56$, $p < 0.05$; 0.5 mg LZP = 1.5 mg LZP: $t_{24} = -0.89$, $p < 0.38$; Figure 2E).The same pattern was observed in the probe interval ($F_{2, 48} = 6.13$, $p < 0.005$; placebo < 0.5 mg LZP: $t_{24} = -2.4$, $p < 0.05$; placebo < 1.5 mg LZP: $t_{24} = -2.89$, $p < 0.05$; 0.5 mg LZP = 1.5 mg LZP: $t_{24} = -1.87$, $p = 0.07$; Figure 2F). Finally, the gamma power in contralateral hemisphere was stronger in comparison with ipsilateral hemisphere, regardless of LZP dose for both the sample arrays (Figure 2G) and the probe arrays (Figure 2H). As control analysis, we tested whether there were systematic gamma power differences between the drug sessions in the baseline interval (−0.5 s to −0.1 s), but this was not the case ($F_{1.1, 26.8} = 1.89$, $p = 0.18$). Despite the strong stimulus-induced gamma power increase, the LZP dosage did not modulate the degree of

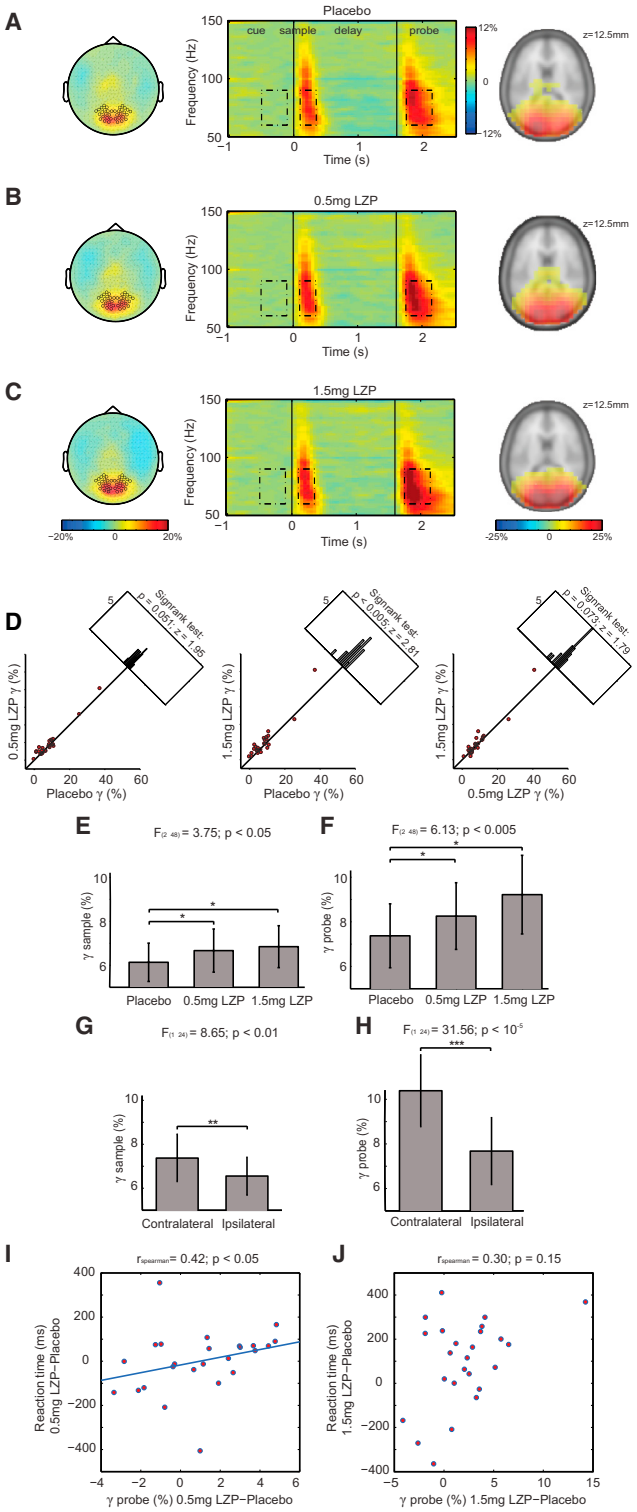

Figure 2. High-Frequency LZP-Induced Power Modulations during the WM Task

(A) Placebo session. Left: topographic representation of the stimulus-induced relative gamma (60–90 Hz) power during the probe interval (1.75–2.15 s). Color code represents relative power changes with respect to the baseline (−0.5 s to −0.1 s). Middle: averaged power time-frequency representations (TFRs) over selected occipital sensors (marked in topographic representations). Time t = 0 s indicates sample array onset. Dashed rectangles indicate the time and frequency selections for the statistical analysis. Right: sources of the gamma band activity obtained using a beamformer approach morphed onto a Montreal Neurological Institute (MNI) standard brain. The peak of the source was in occipital cortex (probe versus baseline; cluster-based nonparametric permutation test, $p < 0.001$, controlled for multiple comparisons). The color code represents the relative power masked by significant grid points within the cluster. The sensors marked in the topographical representations are the sensors of interest used in the subsequent analysis.

(B and C) Stimulus-induced gamma power increase for 0.5 mg lorazepam (LZP) and 1.5 mg LZP, respectively (same conventions as in A).

(D) Scatterplots of the stimulus-induced gamma power; each dot corresponds to a participant. Wilcoxon signed-rank test revealed that the stimulus-induced gamma power increased with LZP dosage. The top right frequency histogram was constructed by summing the scatterplot values within diagonally oriented bins.

(E and F) Repeated-measures ANOVA confirmed that the LZP-induced gamma power increased during both the sample and the probe intervals. Error bars show SEM.

(G and H) The stimulus-induced gamma power was stronger in sensors contralateral to the attended side for both sample and probe periods. Error bars show SEM.

(I) Correlation between drug-related modulations of stimulus-induced gamma power and reaction times. The y axis is the reaction time difference between the 0.5 mg LZP sessions minus the placebo sessions, and the x axis represents the difference between stimulus-induced contralateral gamma power for 0.5 mg LZP minus placebo (each dot represents a participant).

(J) Correlation for 1.5 mg LZP session (same conventions as in I).

*$p < 0.05$, **$p < 0.01$, ***$p < 10^{-5}$.

gamma band modulation as induced by the cue ($F_{2, 48} = 0.25$, $p = 0.77$; Figure S5).

In sum, we found that gamma power during sample and probe increased with LZP dosage. However, the cue-induced hemispheric lateralization in the gamma band did not systematically change with drug.

The Gamma Power that Increased with LZP Predicted Increased Reaction Times

Do the changes in gamma power with LZP explain the changes in behavior? To explore this, we correlated the drug-related changes in gamma power with the drug-related changes in performance. When considering the gamma power in occipital sensors contralateral to the attended visual hemifield, we found a positive correlation with reaction times between 0.5 mg LZP and placebo ($r_{spearman} = 0.42$, $p < 0.05$; Figure 2I). No significant correlations were found between 1.5 mg LZP and reaction time ($r_{spearman} = 0.3$, $p = 0.14$; Figure 2J) or any other behavioral index. Further, we did not find an effect in sensors ipsilateral to the cued hemifield. Summarizing, the increase in reaction time with 0.5 mg LZP dosage (but not with 1.5 mg) was predicted by a drug-related increase of contralateral gamma power in response to the probe.

Gamma Frequency Decreased with LZP

Experiments on hippocampal slices have shown that an increase in inhibitory conductance by pharmacological GABAergic enhancement decreases gamma frequency [4–7]. We sought to test whether this finding generalizes to the human visual stimulus-induced gamma response. To quantify potential frequency changes in the power spectra, we first computed the TFR of the relative change in stimulus-induced gamma during probe presentation (Figure 3A). We observed that the power in the gamma band shifted toward lower frequencies (<75 Hz) with LZP. This is also observed when averaging over the 1.8–1.95 s probe array interval (Figure 3B). To

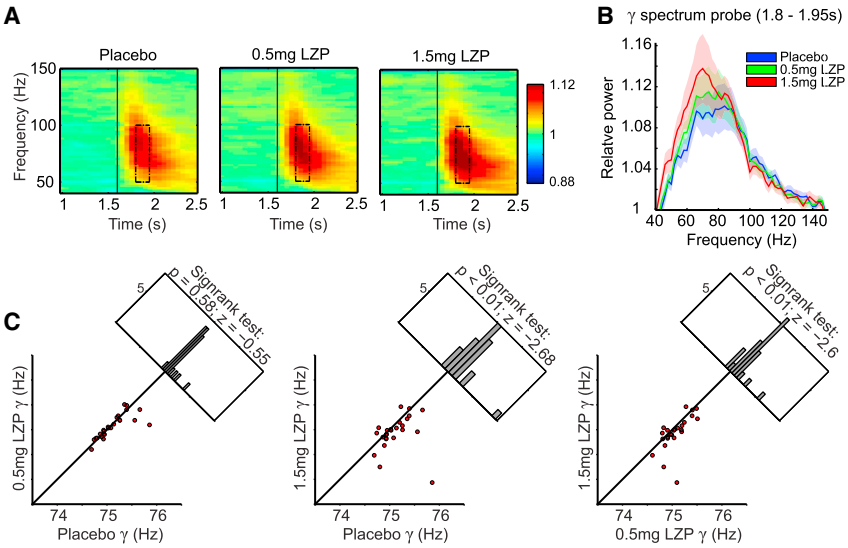

Figure 3. The Gamma Frequency Decreased with LZP Dosage

(A) Induced power TFRs in selected occipital sensors (marked sensors in topography in Figure 4, same conventions) during the probe interval. A relative baseline was applied (−0.5 s to −0.1 s). Time t = 1.6 s indicates probe stimuli onset.

(B) Gamma power spectra computed in the 1.8–1.95 s interval (black rectangles in A) for each drug session.

(C) Scatterplots of the gamma center-of-mass frequency (Hz); each dot represents a participant. Wilcoxon signed-rank test showed a significant gamma frequency decrease with LZP.

quantify this frequency shift, we calculated the "center-of-mass" index (see Supplemental Experimental Procedures) applied to the 50–100 Hz range around the peak in the probe interval defined above. A Wilcoxon signed-rank test revealed that 1.5 mg LZP significantly reduced the gamma frequency in comparison with placebo ($z = -2.68$, $p < 0.01$) and 0.5 mg LZP ($z = -2.6$, $p < 0.01$). We did not observe a difference between 0.5 mg LZP and placebo ($z = -0.55$, $p = 0.58$). We conclude that the dominant frequency in the gamma band frequency decreases with LZP dosage.

As gamma frequency decreases with LZP, one might wonder whether individual gamma frequencies correlate with WM capacity or whether the reduction in WM capacity is predicted by the slowing of the gamma frequency. We addressed this by correlating the gamma frequency (center of mass) with the maximum WM capacity (K_{span}) measured during the behavioral experiment in session 1. There was no significant correlation between K_{span} and gamma frequency in any of the sessions (placebo $r_{spearman} = 0.09$, $p = 0.64$; 0.5 mg LZP $r_{spearman} = 0.07$, $p = 0.73$; 1.5 mg LZP $r_{spearman} = 0.18$, $p = 0.37$). Further, when comparing the drug sessions, there were no significant relationships between the WM capacity reduction and the gamma frequency slowing with neither 0.5 mg LZP ($r_{spearman} = 0.14$, $p = 0.50$) nor 1.5 mg LZP ($r_{spearman} = 0.08$, $p = 0.71$).

LZP Leaves Gamma Activity in Motor Cortex Unaffected

To further determine the brain region specificity of our pharmacological manipulation, we explored the oscillatory dynamics in sensorimotor cortex during the button-press response. Recent human studies have reported on gamma activity in motor cortical areas [20, 21]. To this end, we calculated the TFRs of power, which were time locked to participants' button presses. This revealed gamma activity at the time of the motor response. Contrary to visual areas, the motor-related gamma power was not affected by LZP ($F_{2, 48} = 0.78$, $p = 0.46$; Figure 4). Likewise, absolute gamma power during baseline period (−0.5 s to −0.3 s) was not statistically different ($F_{1.1, 28.5} = 0.85$, $p = 0.81$), discarding the possibility that systematic changes during the premovement period could explain the null effect. These results demonstrate that the pharmacological manipulation specifically affected gamma band activity in the visual cortex.

Modulation of Occipital Alpha Power Is Reduced by LZP

We then set out to examine how brain activity in the lower-frequency bands (<40 Hz) was modulated by LZP. TFRs of power were calculated for individual trials and then averaged with respect to spatial attention condition (left or right) for each MEG session separately. We first considered the modulation with respect to spatial attention. A modulation index (MI) was calculated as the normalized power difference between the attention left versus right trials [22]: $MI = (power_{attention\ left} - power_{attention\ right}) / (power_{attention\ left} + power_{attention\ right})$. Importantly, the same denominator for all drug sessions was used in the normalization (i.e., $power_{attention\ left} + power_{attention\ right}$ from the placebo condition). As shown in Figure 5, alpha band activity was strongly modulated by spatial attention throughout the task. It was reduced contralateral to the direction of attention while it increased relatively over the ipsilateral hemisphere (Figures 5A–5C, left and right columns). Source reconstruction using a beamforming approach revealed that the alpha power was modulated mainly in occipital regions (Figures 5A–5C, center column).

To identify sensors of interest that showed oscillatory power modulations as a function of allocation of attention, we pooled all MEG sessions and conducted a cluster-based nonparametric permutation test applied to the cue period (−1 s to −0.1 s) in the alpha band (9–13 Hz) (see Supplemental Experimental Procedures). For these sensor groups (see Figures 5A–5C, topographical plots, bold circles), we averaged the MI with attention over the left and the right hemisphere (absolute value) and tested the influence of LZP during the delay period (0.5–1.4 s). In addition, we constructed pairwise scatterplots comparing the different drug conditions over participants. These plots revealed that the alpha MI decreased with drug dosage in most participants, as confirmed by the Wilcoxon signed-rank test (Figure 5D). The parametric reduction in modulation with dosage was further confirmed by repeated-measures ANOVA ($F_{1.4, 34.3} = 11.95$, $p < 5 \times 10^{-4}$; placebo > 0.5 mg LZP: $t_{24} = 2.9$, $p < 0.01$; placebo > 1.5 mg LZP: $t_{24} = 3.84$, $p < 0.005$; 0.5 mg LZP > 1.5 mg LZP: $t_{24} = 3.01$, $p < 0.01$; Figure 5E), with both hemispheres being affected by LZP in a nondifferent way. Similar statistical conclusions were found using within-session total power as a denominator ($F_{2, 48} = 6.35$, $p < 0.005$). Complementarily, for each participant, we fitted regression lines to the alpha MI for each session using categorical values (1, 2, and 3) to represent LZP dosages. This resulted in negative slopes significantly different from zero (-0.015 ± 0.004; $t_{24} = -3.84$, $p < 0.001$), supporting the

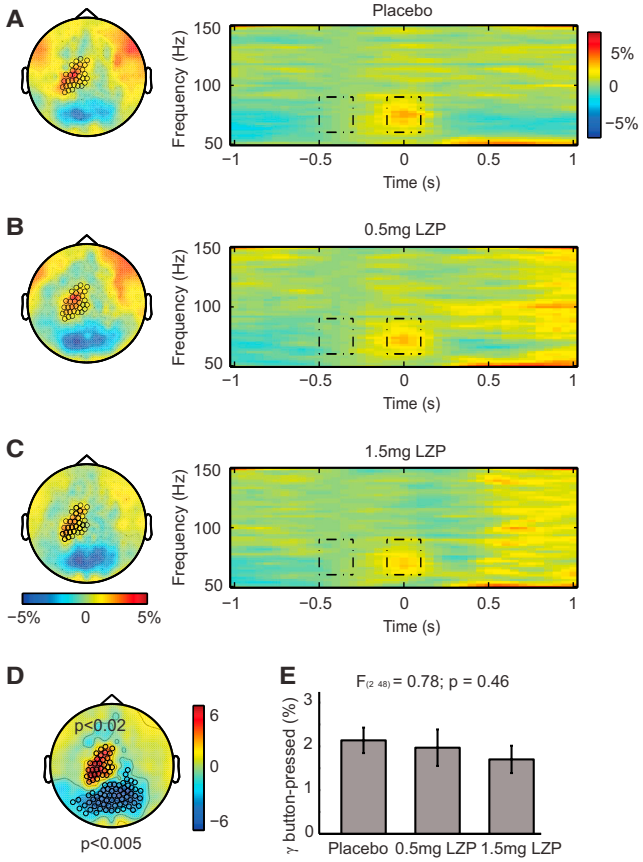

Figure 4. High-Frequency LZP-Induced Power Modulations during Button Press

(A) Left: topography of button-pressed relative gamma power (60–90 Hz) around the button press (−0.1–0.1 s). Color code represents relative changes with respect to the baseline (−0.5 s to −0.3 s). Right: averaged TFRs of power over selected left sensorimotor sensors (marked sensors in topography). Time t = 0 s indicates participant's button press. Dashed lines indicate the baseline interval and button-press period.

(B and C) Induced gamma power for 0.5 mg LZP and 1.5 mg LZP, respectively (same conventions as in A).

(D) Cluster of significant gamma power modulations around the button presses (cluster-based nonparametric permutation test; $p < 0.02$, corrected for multiple comparisons). Color code based on t values when comparing the button press to baseline.

(E) LZP did not modulate sensorimotor gamma power. Error bars show SEM.

notion that the decrease in alpha power with LZP was highly robust.

In short, we found that posterior alpha band activity was modulated as a function of spatial allocation of attention during WM maintenance and that this modulation was reduced with LZP dosage.

The Decrease in Alpha Power Modulations with LZP Predicts WM Impairment

Next, we investigated the modulations in alpha power by LZP in relation to WM performance. To do so, we correlated the drug-related alpha MI changes (combined over hemispheres) with the drug-related performance changes over participants (combined over hemifields). We found a positive correlation between the alpha MI reduction and the decrease in K_{span} when comparing 0.5 mg LZP to placebo ($r_{spearman} = 0.60$, $p < 0.005$; Figure 5F). This was also the case when comparing placebo with 1.5 mg LZP ($r_{spearman} = 0.45$, $p < 0.05$; Figure 5G). To conclude, the participants with the strongest memory-related impairment were the ones with the strongest alpha MI reductions.

LZP Interacts with Alpha Power in Ipsilateral and Contralateral Hemispheres

Is the decrease in alpha MI by LZP mainly explained by alpha modulations in the hemisphere ipsilateral or contralateral to the cued hemifield? WM impairment could be a consequence of a failure to inhibit distracting visual information as reflected by ipsilateral alpha power. To investigate this issue, we computed the absolute alpha power in ipsilateral and contralateral sensors during the delay interval for all dosages separately. This revealed that the absolute alpha power during the delay interval in ipsilateral hemisphere was stronger than that in contralateral hemisphere ($F_{1, 24} = 35.5$, $p < 5 \times 10^{-6}$; Figure 6). Strikingly, as seen in Figure 6, the 3 × 2 repeated-measures ANOVA revealed a significant drug × hemisphere interaction ($F_{1.6\ 38.4} = 6.07$, $p < 0.01$; Figures 6D and 6E), suggesting that LZP impacted alpha power in ipsilateral hemisphere differently compared to contralateral hemisphere. This was explained by LZP strongly reducing the alpha power in the ipsilateral hemisphere to the cued visual hemifield (ipsi placebo > ipsi 0.5 mg LZP: $t_{24} = 3.15$, $p < 0.01$; ipsi placebo > ipsi10.5 mg LZP: $t_{24} = 6.43$, $p < 5 \times 10^{-6}$; ipsi 0.5 mg LZP > ipsi 1.5 mg LZP: $t_{24} = 5.09$, $p < 10^{-4}$) in comparison to the contralateral power (contra placebo > contra 0.5 mg LZP: $t_{24} = 2.26$, $p < 0.05$; contra placebo > contra 1.5 mg LZP: $t_{24} = 4.44$, $p < 5 \times 10^{-4}$; contra 0.5 mg LZP > contra 1.5 mg LZP: $t_{24} = 5.28$, $p < 5 \times 10^{-5}$; Figures 6D and 6E). The present interaction was specific to the delay interval; it was not observed in the cue interval ($F_{2, 48} = 0.82$, $p = 0.44$).

As for alpha MI, for each participant, we fitted regression lines to ipsilateral and contralateral hemispheric alpha power using categorical values to represent LZP concentrations. Both the ipsilateral (-0.07 ± 0.01; $t_{24} = -6.43$, $p < 5 \times 10^{-6}$) and contralateral (-0.06 ± 0.01; $t_{24} = -5.28$, $p < 5 \times 10^{-5}$) slopes were significantly different from zero. Importantly, the regression slopes were significantly more negative in sensors in the ipsilateral hemisphere compared to the contralateral hemisphere ($t_{24} = -2.82$, $p < 0.01$). We also tested whether the absolute power correlated with the alpha MI over subjects; this was not the case. In addition, the individual drug-related changes in alpha MI did not correlate with the drug-related changes in absolute alpha power during the delay interval.

In sum, LZP reduced alpha power in the ipsilateral hemisphere more so than in the contralateral hemisphere during the delay interval of the WM task.

Gamma and Alpha Attentional Power Modulations Correlate over Participants

So far, we have demonstrated that gamma and alpha power are modulated as a function of spatial attention (Figures S4 and 5A–5C, respectively). Does the alpha modulation in the delay interval predict the gamma modulation during the probe delay? To test this, we correlated over participants the alpha MI during the delay interval with the gamma MI during the probe interval for each MEG session separately (using the MIs combined over hemispheres). We found a significant negative correlation during placebo ($r_{spearman} = -0.42$, $p < 0.05$) and 1.5 mg LZP ($r_{spearman} = -0.42$, $p < 0.05$), but not during 0.5 mg LZP ($r_{spearman} = -0.31$, $p = 0.13$; Figure S6). This

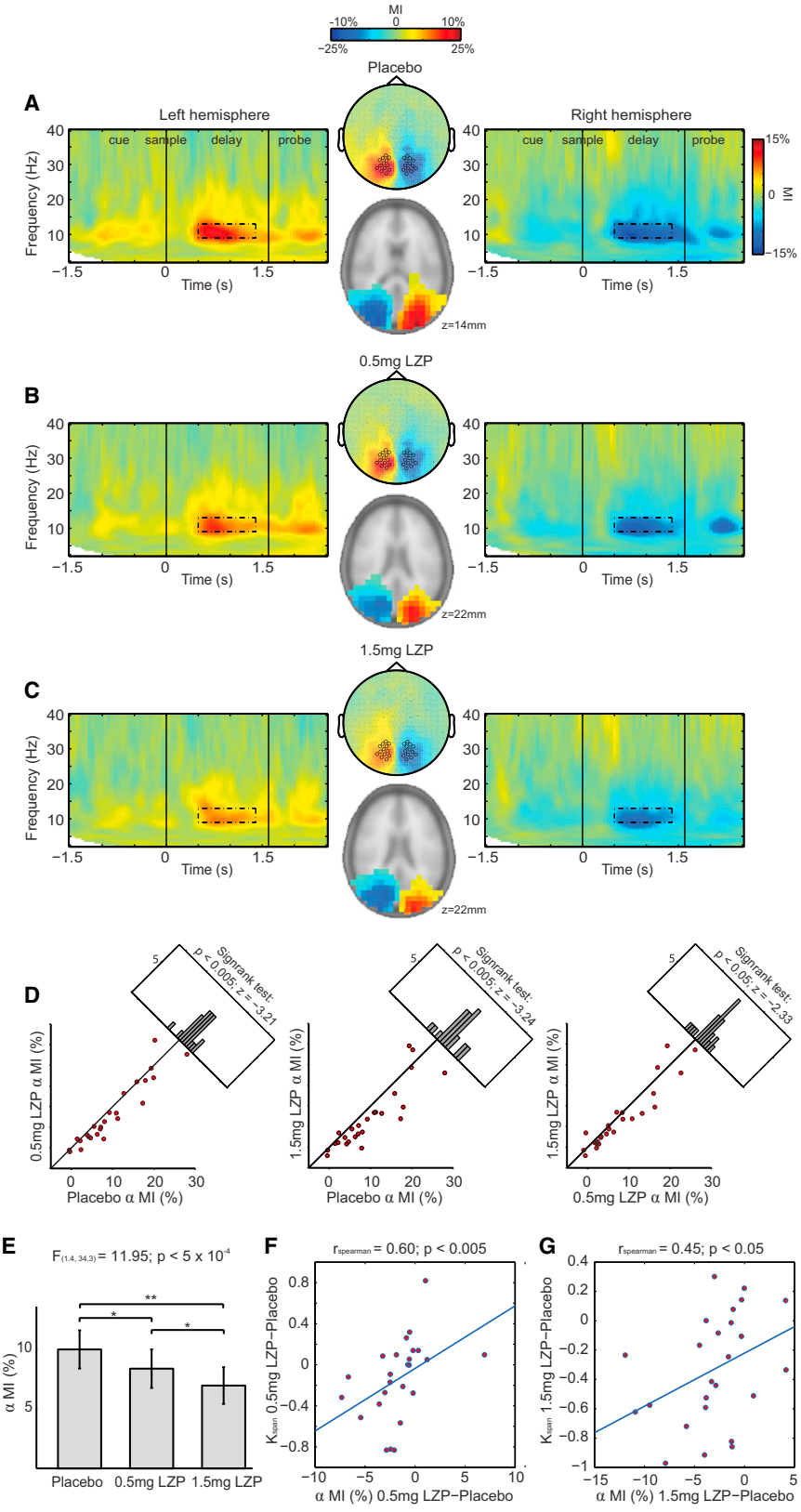

Figure 5. Low-Frequency LZP-Induced Power Modulations during WM Task

(A) Placebo session. Averaged TFRs shown by the alpha modulation index (MI) over left and right occipital sensors (marked sensors in topography). Color code represents the modulation in power with attention (normalized difference for left minus right attention). Time t = 0 s indicates sample array onset. Middle above: MI topography for the time and frequency ranges indicated by the dashed rectangles (9–13 Hz; 0.5–1.4 s). Middle below: alpha sources producing the MI obtained with a beamforming approach morphed to an MNI standard brain. The peak of the source was located in occipital cortex (attention left versus attention right; cluster-based nonparametric permutation test; $p < 0.02$, controlled for multiple comparisons). The color code represents the alpha MI of significant grid points. The marked sensors were used in the subsequent analysis.

(B and C) The alpha MI for 0.5 mg LZP and 1.5 mg LZP, respectively (same conventions as in A).

(D) Scatterplots of the alpha MI during the delay period; each dot corresponds to a participant. Wilcoxon signed-rank tests shows that the alpha MI significantly decreased with LZP dosage.

(E) The main effect during and alpha MI show a highly robust decrease. Error bars show SEM.

(F) Participants with a strong drug-related decrease in alpha MI were also participants with a strong decrease in WM capacity. The y axis represents the K_{span} difference between the 0.5 mg LZP sessions minus the placebo sessions, and the x axis represents the difference between alpha MIs for 0.5 mg LZP minus placebo (each dot represents a participant).

(G) Correlation for 1.5 mg LZP session (same conventions as in G).

*p < 0.01, **p < 0.005.

means that the participants with a stronger alpha power modulation during retention (positive MI) are also those with a stronger gamma power modulation in the reverse direction during probe processing (negative MI). These findings suggest that alpha band modulation reflects top-down control, which is predictive of the gamma band activity reflecting feedforward processing.

Discussion

We used MEG to investigate how the GABAergic allosteric modulator LZP influences human oscillatory brain activity during WM operations. We show for the first time in humans that stimulus-induced gamma power increases while frequency decreases due to the enhancement of inhibitory conductance by the selective enhancement of $GABA_A$ receptors. The drug-related increase in occipital gamma power contralateral to the attended hemifield was predictive of increases in response times. Even though LZP modulates $GABA_A$ receptors brain-wide, sensorimotor gamma activity was not modulated by LZP, i.e., the effect in the gamma band was specific to the visual cortex. Oscillations in the alpha band were strongly lateralized according to direction of attention during the memory delay: they decreased in

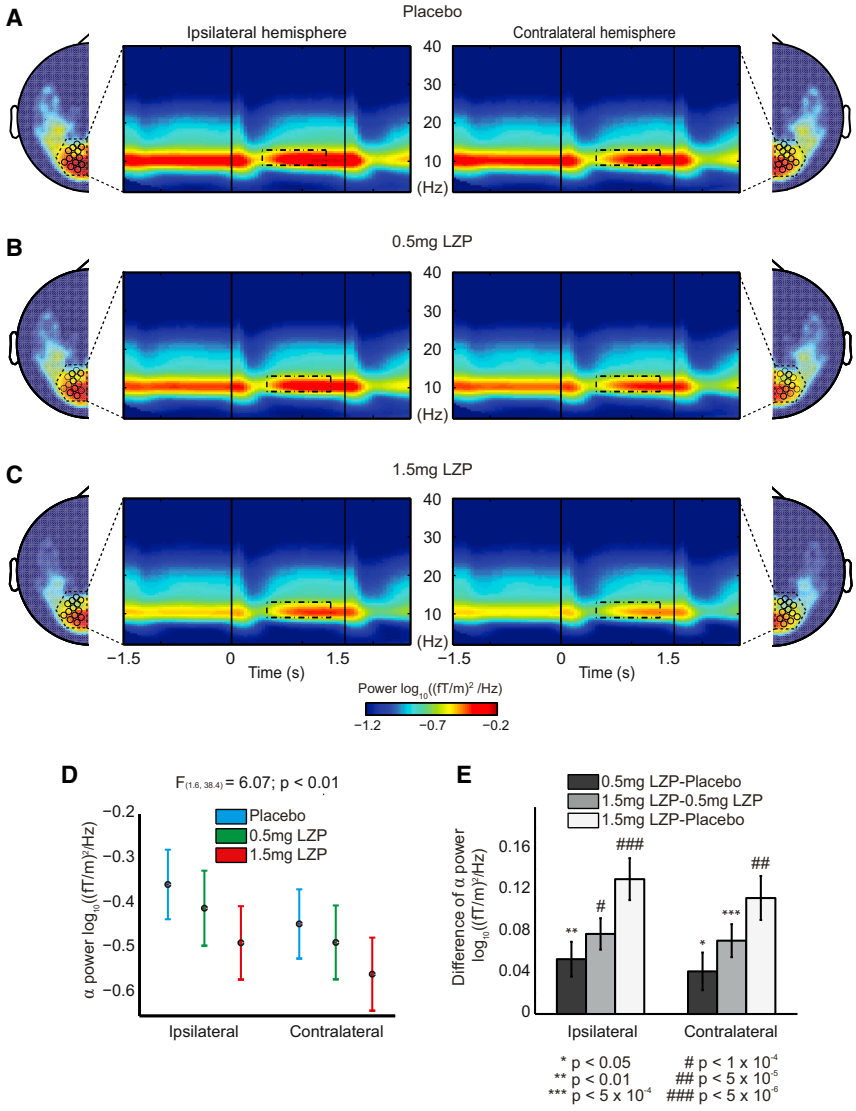

Figure 6. Drug-Related Alpha Power Changes in the Hemispheres Contralateral and Ipsilateral to the Cued Direction

(A) Placebo session. Left: absolute power in the hemisphere ipsilateral to the attended visual field. Both topographic plots (delay period: 0.5–1.4 s; alpha power: 9–13 Hz) and TFRs represent power for occipital sensors shown (marked in topographical plot). Time t = 0 s indicates sample array onset. Right: similar plots for effects contralateral to the attended visual hemifield.

(B and C) 0.5 mg and 1.5 mg LZP sessions, respectively (same conventions as in A).

(D) The absolute alpha power during the delay period decreased systematically with drug in both the hemisphere contralateral to the cue and the hemisphere ipsilateral to the cue. Further, the decrease ipsilateral to the cue was stronger than the decrease contralateral to the cue, yielding a significant interaction, as revealed by repeated-measures ANOVA. Error bars show SEM.

(E) The difference in absolute alpha power when comparing the different drug conditions for contralateral and ipsilateral hemisphere to cue. A pairwise post hoc t test showed that alpha absolute power in the ipsilateral hemisphere was more suppressed with LZP in comparison to the contralateral hemisphere. Error bars show SEM.

occipital regions contralateral to the side of the cued memory array, whereas they increased relatively in ipsilateral regions. The alpha band lateralization was reduced with LZP dosage, and furthermore, it predicted WM performance. Our findings strongly implicate GABAergic interneurons in the regulation and generation of gamma and alpha activity, respectively, during human WM operations.

GABAergic Modulations of Gamma Oscillations

Our findings show that human visual gamma power and frequency are modulated by an increase in $GABA_A$ neurotransmission. Although previous studies have implicated GABA in generating gamma band activity associated with visual stimulation, the findings are mixed. Recent MEG studies reported a gamma power increase with the $GABA_A$ receptor agonist propofol [23], but not with the GABA reuptaker inhibitor tiagabine [24]. The decrease in gamma frequency with LZP has not been reported in other studies applying GABAergic allosteric modulators in humans [23, 24] but has been shown in rat and monkey visual cortex under anesthesia [25, 26]. In addition, the administration of alcohol (GABA and NMDA modulator) did produce a decrease in gamma frequency during visual stimulation [27]. Finally, a recent study combining magnetic resonance spectroscopy (MRS) and MEG found a relationship between gamma frequency and GABA concentration [28], although the reliability of the findings have been challenged very recently [29].

In our study, sensorimotor gamma power changes locked to the button press were not modulated by the drug [20, 21]. In a recent study on humans in which acetylcholine was enhanced, an effect on gamma power in visual, but not sensorimotor, regions was reported [30]. Furthermore, it should be emphasized that the concentration of GABA receptors is disproportionally high in the occipital cortex, as measured by PET [31]. We concluded that the physiological mechanisms of sensorimotor gamma activity differ from the mechanisms of visual gamma activity. As such, our findings are the first to report a robust increase in gamma band activity in a WM task associated with a frequency decrease due to $GABA_A$ enhancement.

Which mechanisms might explain the increase in gamma power and the decrease in frequency with LZP? The physiological mechanisms behind gamma oscillations have been extensively studied by in vitro work in the rat hippocampus [2, 3]. This work has demonstrated that GABAergic interneurons play a critical role for the rhythmic synchronization on neuronal populations in the gamma band. It has been demonstrated that gamma power increases as a function of IPSP ([4–6], but see [7]). Also, the increases in IPSPs result in a prolongation of the gamma cycle, thus reducing the gamma frequency [4–7]. Two mechanisms have been proposed for generating gamma oscillations: the interneuronal network gamma (ING) and the pyramidal-interneuronal network gamma (PING) mechanism. In ING models, inhibitory

interneurons are necessary and sufficient for generating gamma oscillations [6], whereas in PING, the gamma oscillations are a consequence of the interplay between pyramidal and inhibitory interneurons [32]. Because MEG recordings cannot tell cell types apart [33], we cannot distinguish whether a PING or an ING mechanism dominates. However, in a recent nonhuman primate study, Vinck et al. [34] analyzed intracranially recorded single-unit activity in association with gamma oscillations in V4. They applied a spike-waveform analysis to sort the cells in broad spiking (BS) and narrow spiking (NS) neurons, i.e., putative pyramidal neurons and inhibitory cells, respectively. The firing BS neurons preceded the NS neurons by 3.3 ms while both were locked to the phase of the gamma as identified in the local field potential. This finding supports the PING model and might generalize to the human gamma band activity.

The Functional Role of Gamma Oscillations

We observed that gamma band activity was strongest contralateral to the direction of attention during visual stimulation. Previously, studies have implicated gamma oscillations in visual processing and neuronal communication [35]. For instance, it has been proposed that gamma band synchronization results in a stronger feedforward drive to downstream visual regions [36–38]. We propose that the gamma band synchronization we observed during the sample and probe intervals reflects encoding and recall of the attended memory array involving early visual areas. Importantly, the increase in gamma power with LZP does not predict better performance. We conclude that although the gamma band synchronization might reflect the encoding visual stimuli, it does not necessarily mean that more gamma power is predictive of better performance.

GABAergic Modulation of Alpha Oscillations

It is well established that alpha power recorded during rest is reduced with GABAergic agonists ([13, 14], but see [39, 40]). We now extend these findings by demonstrating that the modulation of alpha power also is robustly reduced during WM maintenance. High alpha power has been proposed to reflect reduced vigilance. Because we find that LZP decreases alpha power while performance is reduced, it is clear that the magnitude of alpha power does not simply equate lack of vigilance.

What are the mechanisms explaining the decrease in alpha power with LZP? One simple explanation is that LZP increases GABAergic inhibition and reduces the pyramidal firing without affecting oscillatory frequency per se. This interpretation is consistent with an in vitro study applying diazepam: although this GABAergic agonist decreases the number of spikes per burst, it leaves the burst rate unaffected [41]. Another not mutually exclusive possibility is the involvement of the thalamus in the generation of alpha oscillations. Whereas the alpha activity measured with MEG is most likely produced by sources in the deeper layers of neocortex [42, 43], the neocortical alpha sources have been found to be coupled to thalamic generators [12, 44, 45]. These findings have been used to constrain physiologically realistic computational models of the alpha rhythm [46]. As such, the modulation in alpha activity with LZP might have a thalamic origin as well.

Given the proposed inhibitory role of the alpha band activity [15, 16], one might have expected the alpha power to increase as the GABAergic inhibition increases. Because we obtained the reverse finding, the dynamics are evidently more complicated than that. Future intracranial animal recordings would be required to gain full insight into this issue.

In future research, it would be interesting to uncover whether it is actually the GABAergic modulation of frontal or subcortical sources causing the changes in posterior alpha band activity. Given that it is problematic to detect deeper sources with MEG, this could be done in a combined EEG/fMRI. Drug-specific effects in relation to the alpha activity could then be investigated in regions potentially involved in the control of the alpha activity (dorsal attention network, pulvinar, and striatum).

The Functional Role of the Alpha Band Oscillations

It has been proposed that alpha band activity reflects the allocation of computational resources [15, 16]. Basically, a regional-specific increase in alpha power reflects functional inhibition, whereas a decrease reflects engagement. This inhibition might be crucial for distracter suppression, ensuring the integrity of the WM representations [47, 48]. Our findings are fully consistent with this notion. Consistently, LZP produced a stronger reduction in alpha power suppression over ipsilateral hemisphere in comparison with the suppression in contralateral hemisphere during the delay period, not during the cue. We interpret this finding as a pharmacological task-specific effect on alpha oscillations that cannot be accounted for by a general decrease in vigilance (i.e., the same power decrease would be expected in ipsilateral and contralateral hemispheres).

Conclusions

Altogether, the results presented here suggest that the same GABAergic physiological mechanism for neuronal gamma oscillations uncovered by hippocampal rat models applies to human visual brain oscillations during WM processing. Because the modulations in the alpha band were present during the cue and delay intervals, we propose that alpha oscillations reflect top-down processing (see also [38]). The gamma band activity mainly occurred during the presentation of the memory array and probe and is therefore likely to be dominated by feedforward processing. Our data underscore an important role of GABAergic neurotransmission for neuronal synchronization on both gamma and alpha band oscillations. As such, our findings bring us an important step closer to linking neuronal dynamics to human behavior by embracing established animal models.

Experimental Procedures

Thirty-two healthy participants gave informed consent approved by the local research ethics committee (Commissie Mensgebonden Onderzoek; Arnhem-Nijmegen, number: 2011/199, date: August 5, 2011) and were compensated for their participation. Data from seven participants were rejected (see Supplemental Experimental Procedures for rejection criteria), leaving a total of 25 participants. They were all right-handed and had normal or corrected-to-normal vision (mean age: 22.4, range: 18–28 years old, 12 males; see Supplemental Experimental Procedures and Figure 1A for complete experimental design and general pharmacological procedure).

We adapted a classical delayed match-to-sample visuospatial WM task [18] while ongoing brain activity was recorded using a whole-head MEG system with 275 axial gradiometers (VSM/CTF Systems). Data were analyzed offline using FieldTrip [49] (http://fieldtrip.fcdonders.nl/), an open-source toolbox developed at the Donders Institute for Brain, Cognition, and Behavior, and custom MATLAB code (MathWorks).

Supplemental Information

Supplemental Information includes Supplemental Experimental Procedures and six figures and can be found with this article online at http://dx.doi.org/10.1016/j.cub.2014.10.017.

Acknowledgments

This work was supported by the Netherlands Organization for Scientific Research, by an Open Competition/MaGW grant (grant number 400-09-491 to D.L.-S., R.C., and O.J.), and by a VICI grant (grant number 453-09-002 to O.J.). We thank Paul Gaalman and Rene Scheeringa for assistance with MRI collection; Sander Berends for assistance with MEG recordings; and Arjen Stolk for assistance with the real-time head localizer tool.

Received: August 9, 2014
Revised: October 5, 2014
Accepted: October 8, 2014
Published: November 26, 2014

References

1. Wang, X.-J. (2010). Neurophysiological and computational principles of cortical rhythms in cognition. Physiol. Rev. *90*, 1195–1268.
2. Bartos, M., Vida, I., and Jonas, P. (2007). Synaptic mechanisms of synchronized gamma oscillations in inhibitory interneuron networks. Nat. Rev. Neurosci. *8*, 45–56.
3. Traub, R.D., Whittington, M.A., and Jefferis, J.G.R. (1999). Fast Oscillations in Cortical Circuits (Cambridge: MIT press).
4. Traub, R.D., Whittington, M.A., Colling, S.B., Buzsáki, G., and Jefferys, J.G. (1996). Analysis of gamma rhythms in the rat hippocampus in vitro and in vivo. J. Physiol. *493*, 471–484.
5. Whittington, M.A., Jefferys, J.G., and Traub, R.D. (1996). Effects of intravenous anaesthetic agents on fast inhibitory oscillations in the rat hippocampus in vitro. Br. J. Pharmacol. *118*, 1977–1986.
6. Whittington, M.A., Traub, R.D., and Jefferys, J.G.R. (1995). Synchronized oscillations in interneuron networks driven by metabotropic glutamate receptor activation. Nature *373*, 612–615.
7. Faulkner, H.J., Traub, R.D., and Whittington, M.A. (1998). Disruption of synchronous gamma oscillations in the rat hippocampal slice: a common mechanism of anaesthetic drug action. Br. J. Pharmacol. *125*, 483–492.
8. Fries, P., Nikolić, D., and Singer, W. (2007). The gamma cycle. Trends Neurosci. *30*, 309–316.
9. Fries, P., Reynolds, J.H., Rorie, A.E., and Desimone, R. (2001). Modulation of oscillatory neuronal synchronization by selective visual attention. Science *291*, 1560–1563.
10. Womelsdorf, T., Fries, P., Mitra, P.P., and Desimone, R. (2006). Gamma-band synchronization in visual cortex predicts speed of change detection. Nature *439*, 733–736.
11. Chalk, M., Herrero, J.L., Gieselmann, M.A., Delicato, L.S., Gotthardt, S., and Thiele, A. (2010). Attention reduces stimulus-driven gamma frequency oscillations and spike field coherence in V1. Neuron *66*, 114–125.
12. Lőrincz, M.L., Kékesi, K.A., Juhász, G., Crunelli, V., and Hughes, S.W. (2009). Temporal framing of thalamic relay-mode firing by phasic inhibition during the alpha rhythm. Neuron *63*, 683–696.
13. Schreckenberger, M., Lange-Asschenfeldt, C., Lochmann, M., Mann, K., Siessmeier, T., Buchholz, H.-G., Bartenstein, P., and Gründer, G. (2004). The thalamus as the generator and modulator of EEG alpha rhythm: a combined PET/EEG study with lorazepam challenge in humans. Neuroimage *22*, 637–644.
14. Ahveninen, J., Lin, F.H., Kivisaari, R., Autti, T., Hämäläinen, M., Stufflebeam, S., Belliveau, J.W., and Kähkönen, S. (2007). MRI-constrained spectral imaging of benzodiazepine modulation of spontaneous neuromagnetic activity in human cortex. Neuroimage *35*, 577–582.
15. Klimesch, W. (2012). α-band oscillations, attention, and controlled access to stored information. Trends Cogn. Sci. *16*, 606–617.
16. Jensen, O., and Mazaheri, A. (2010). Shaping functional architecture by oscillatory alpha activity: gating by inhibition. Front Hum Neurosci *4*, 186.
17. Riss, J., Cloyd, J., Gates, J., and Collins, S. (2008). Benzodiazepines in epilepsy: pharmacology and pharmacokinetics. Acta Neurol. Scand. *118*, 69–86.
18. Vogel, E.K., and Machizawa, M.G. (2004). Neural activity predicts individual differences in visual working memory capacity. Nature *428*, 748–751.
19. Stolk, A., Todorovic, A., Schoffelen, J.-M., and Oostenveld, R. (2013). Online and offline tools for head movement compensation in MEG. Neuroimage *68*, 39–48.
20. Hall, S.D., Stanford, I.M., Yamawaki, N., McAllister, C.J., Rönnqvist, K.C., Woodhall, G.L., and Furlong, P.L. (2011). The role of GABAergic modulation in motor function related neuronal network activity. Neuroimage *56*, 1506–1510.
21. Muthukumaraswamy, S.D., Myers, J.F.M., Wilson, S.J., Nutt, D.J., Lingford-Hughes, A., Singh, K.D., and Hamandi, K. (2013). The effects of elevated endogenous GABA levels on movement-related network oscillations. Neuroimage *66*, 36–41.
22. Thut, G., Nietzel, A., Brandt, S.A., and Pascual-Leone, A. (2006). α-band electroencephalographic activity over occipital cortex indexes visuospatial attention bias and predicts visual target detection. J. Neurosci. *26*, 9494–9502.
23. Saxena, N., Muthukumaraswamy, S.D., Diukova, A., Singh, K., Hall, J., and Wise, R. (2013). Enhanced stimulus-induced gamma activity in humans during propofol-induced sedation. PLoS ONE *8*, e57685.
24. Muthukumaraswamy, S.D., Myers, J.F.M., Wilson, S.J., Nutt, D.J., Hamandi, K., Lingford-Hughes, A., and Singh, K.D. (2013). Elevating endogenous GABA levels with GAT-1 blockade modulates evoked but not induced responses in human visual cortex. Neuropsychopharmacology *38*, 1105–1112.
25. Xing, D., Shen, Y., Burns, S., Yeh, C.-I., Shapley, R., and Li, W. (2012). Stochastic generation of gamma-band activity in primary visual cortex of awake and anesthetized monkeys. J. Neurosci. *32*, 13873–80a.
26. Oke, O.O., Magony, A., Anver, H., Ward, P.D., Jiruska, P., Jefferys, J.G.R., and Vreugdenhil, M. (2010). High-frequency gamma oscillations coexist with low-frequency gamma oscillations in the rat visual cortex in vitro. Eur. J. Neurosci. *31*, 1435–1445.
27. Campbell, A.E., Sumner, P., Singh, K.D., and Muthukumaraswamy, S.D. (2014). Acute effects of alcohol on stimulus-induced gamma oscillations in human primary visual and motor cortices. Neuropsychopharmacology *39*, 2104–2113.
28. Muthukumaraswamy, S.D., Edden, R.A., Jones, D.K., Swettenham, J.B., and Singh, K.D. (2009). Resting GABA concentration predicts peak gamma frequency and fMRI amplitude in response to visual stimulation in humans. Proc. Natl. Acad. Sci. USA *106*, 8356–8361.
29. Cousijn, H., Haegens, S., Wallis, G., Near, J., Stokes, M.G., Harrison, P.J., and Nobre, A.C. (2014). Resting GABA and glutamate concentrations do not predict visual gamma frequency or amplitude. Proc. Natl. Acad. Sci. USA *111*, 9301–9306.
30. Bauer, M., Kluge, C., Bach, D., Bradbury, D., Heinze, H.J., Dolan, R.J., and Driver, J. (2012). Cholinergic enhancement of visual attention and neural oscillations in the human brain. Curr. Biol. *22*, 397–402.
31. Gründer, G., Siessmeier, T., Lange-Asschenfeldt, C., Vernaleken, I., Buchholz, H.-G., Stoeter, P., Drzezga, A., Lüddens, H., Rösch, F., and Bartenstein, P. (2001). [^{18}F]Fluoroethylflumazenil: a novel tracer for PET imaging of human benzodiazepine receptors. Eur. J. Nucl. Med. *28*, 1463–1470.
32. Tiesinga, P., and Sejnowski, T.J. (2009). Cortical enlightenment: are attentional gamma oscillations driven by ING or PING? Neuron *63*, 727–732.
33. Hämäläinen, M., Hari, R., Ilmoniemi, R.J., Knuutila, J., and Lounasmaa, O.V. (1993). Magnetoencephalography - theory, instrumentation, and applications to noninvasive studies of the working human brain. Rev. Mod. Phys. *65*, 413–497.
34. Vinck, M., Womelsdorf, T., Buffalo, E.A., Desimone, R., and Fries, P. (2013). Attentional modulation of cell-class-specific gamma-band synchronization in awake monkey area v4. Neuron *80*, 1077–1089.
35. Fries, P. (2005). A mechanism for cognitive dynamics: neuronal communication through neuronal coherence. Trends Cogn. Sci. *9*, 474–480.
36. Bosman, C.A., Schoffelen, J.M., Brunet, N., Oostenveld, R., Bastos, A.M., Womelsdorf, T., Rubehn, B., Stieglitz, T., De Weerd, P., and Fries, P. (2012). Attentional stimulus selection through selective synchronization between monkey visual areas. Neuron *75*, 875–888.
37. Grothe, I., Neitzel, S.D., Mandon, S., and Kreiter, A.K. (2012). Switching neuronal inputs by differential modulations of gamma-band phase-coherence. J. Neurosci. *32*, 16172–16180.
38. van Kerkoerle, T., Self, M.W., Dagnino, B., Gariel-Mathis, M.-A., Poort, J., van der Togt, C., and Roelfsema, P.R. (2014). Alpha and gamma oscillations characterize feedback and feedforward processing in monkey visual cortex. Proc. Natl. Acad. Sci. USA *111*, 14332–14341.

39. Hall, S.D., Barnes, G.R., Furlong, P.L., Seri, S., and Hillebrand, A. (2010). Neuronal network pharmacodynamics of GABAergic modulation in the human cortex determined using pharmaco-magnetoencephalography. Hum. Brain Mapp. *31*, 581–594.
40. Jensen, O., Goel, P., Kopell, N., Pohja, M., Hari, R., and Ermentrout, B. (2005). On the human sensorimotor-cortex beta rhythm: sources and modeling. Neuroimage *26*, 347–355.
41. Antkowiak, B. (1999). Different actions of general anesthetics on the firing patterns of neocortical neurons mediated by the GABA(A) receptor. Anesthesiology *91*, 500–511.
42. Spaak, E., Bonnefond, M., Maier, A., Leopold, D.A., and Jensen, O. (2012). Layer-specific entrainment of γ-band neural activity by the α rhythm in monkey visual cortex. Curr. Biol. *22*, 2313–2318.
43. Lopes Da Silva, F.H., and Storm Van Leeuwen, W. (1977). The cortical source of the alpha rhythm. Neurosci. Lett. *6*, 237–241.
44. Saalmann, Y.B., Pinsk, M.A., Wang, L., Li, X., and Kastner, S. (2012). The pulvinar regulates information transmission between cortical areas based on attention demands. Science *337*, 753–756.
45. Lopes da Silva, F.H., Vos, J.E., Mooibroek, J., and Van Rotterdam, A. (1980). Relative contributions of intracortical and thalamo-cortical processes in the generation of alpha rhythms, revealed by partial coherence analysis. Electroencephalogr. Clin. Neurophysiol. *50*, 449–456.
46. Vijayan, S., Ching, S., Purdon, P.L., Brown, E.N., and Kopell, N.J. (2013). Thalamocortical mechanisms for the anteriorization of α rhythms during propofol-induced unconsciousness. J. Neurosci. *33*, 11070–11075.
47. Sauseng, P., Klimesch, W., Heise, K.F., Gruber, W.R., Holz, E., Karim, A.A., Glennon, M., Gerloff, C., Birbaumer, N., and Hummel, F.C. (2009). Brain oscillatory substrates of visual short-term memory capacity. Curr. Biol. *19*, 1846–1852.
48. Bonnefond, M., and Jensen, O. (2012). Alpha oscillations serve to protect working memory maintenance against anticipated distracters. Curr. Biol. *22*, 1969–1974.
49. Oostenveld, R., Fries, P., Maris, E., and Schoffelen, J.-M. (2011). FieldTrip: open source software for advanced analysis of MEG, EEG, and invasive electrophysiological data. Comput. Intell. Neurosci. *2011*, 156869.